Transition-Metal Nanocluster Stabilization versus Agglomeration Fundamental Studies: Measurement of the Two Types of Rate Constants for Agglomeration Plus Their Activation Parameters under Catalytic Conditions

Lisa Starkey Ott and Richard G. Finke*

Colorado State University, Department of Chemistry, Fort Collins, Colorado 80523

Received August 24, 2006. Revised Manuscript Received September 7, 2007

A recent mechanistic study of transition-metal nanocluster formation and agglomeration (Besson, C.; Finney, E. E.; Finke, R. G. *J. Am. Chem. Soc.* **2005**, *127*, 8179) identified two types of agglomeration for the first time, specifically bimolecular agglomeration of nanoclusters B (i.e., B + B → C; rate constant k_3) and a new step of autocatalytic agglomeration of nanoclusters B with larger already somewhat agglomerated nanoclusters and/or bulk metal, C (i.e., B + C → 1.5C; rate constant k_4). Herein, this two-step, parallel-path agglomeration mechanism is independently tested by the temperature-induced agglomeration of the prototype preformed, pre-isolated $P_2W_{15}Nb_3O_{62}^{9-}$-stabilized $Ir(0)_{\sim 900}$ transition-metal nanoclusters undergoing cyclohexene hydrogenation and concomitant agglomeration. The resulting k_3 and k_4 rate constants are measured as a function of the temperature, yielding the previously unavailable $\Delta H^{\ddagger}$ and $\Delta S^{\ddagger}$ for each type of nanocluster agglomeration under the specific reaction conditions, which include the presence of cyclohexene and H_2, $\Delta H_3^{\ddagger} = 6.2(3)$ kcal/mol, $\Delta S_3^{\ddagger} = -46(2)$ eu and $\Delta H_4^{\ddagger} = 18(1)$ kcal/mol and $\Delta S_4^{\ddagger} = -2.5(2)$ eu (standard state = 1 M). The interesting activation parameters suggest that the k_3 agglomeration step may be associatively activated, while the k_4 step appears to be dissociatively activated, for reasons discussed in the main text. Also reported is the attempted agglomeration of preformed, isolated $Ir(0)_{\sim 900}$ nanoclusters with added salt, $[Bu_4N][BF_4]$. Reported primarily in the Supporting Information are extensive efforts attempting to achieve the in-principle ideal goal of measuring agglomeration kinetics (k_3 and k_4) simultaneously with nucleation and growth kinetics (k_1 and k_2) in the presence of pyridine as a known agglomerating agent. Overall, the successful kinetic measurements of the k_3 and k_4 agglomeration steps for pre-isolated $Ir(0)_{\sim 900}$ nanoclusters provided herein are significant in seven ways: (i) they independently verify the only recently discovered two types of agglomeration, bimolecular (k_3) and autocatalytic (k_4) agglomeration; (ii) the temperature dependence of the k_3 and k_4 processes provide the first activation parameters for these processes and yield the previously unavailable insights of their apparently associatively activated (k_3) and dissociatively activated (k_4) natures, at least under the reaction conditions with olefin and hydrogen present; and (iii) the two rate constants k_3 and k_4 define the term "nanocluster stability" in solution rigorously and in an experimentally testable way for the first time. In addition, (iv) the present studies serve as "proof of concept" that the measurement of agglomeration rate constants is a viable way to rank quantitatively and therefore distinguish transition-metal nanocluster stabilizers; (v) the results show that added salts, such as $[Bu_4N][BF_4]$, are ineffective in agglomerating at least highly stabilized $P_2W_{15}Nb_3O_{62}^{9-}$-ligated $Ir(0)_{\sim 900}$ nanoclusters; and (vi) the results give some insight into the relative sizes of agglomerated C ($\geq Ir(0)_{\sim 2000}$) versus that of the starting $Ir(0)_{\sim 900}$ nanoclusters, B. Finally, (vii) the results also make apparent that the study of nanocluster agglomeration, by additional physical methods and using other, to-be-developed agglomerants, as a preferred way to quantitate nanocluster stability, remains as an important research challenge. Some thoughts about what additional physical methods may provide the best avenues for future studies are briefly discussed in the Summary.

Introduction

Nanocluster chemistry is of enormous current interest[1–7] for applications as wide and varied as quantum dots,[8] chemical sensors,[9] components in industrial lithography,[10] and catalysis.[11] In the literature, a myriad-indeed what has been called a "dizzying variety"[6]-of anions,[12–14] solvents,[15–17] polymers,[18–20] dendrimers,[21–23] siloxanes,[24] and other entities (including reverse micelles,[25] ionic liquids,[26–28] and resorcinarene molecules,[29,30]to mention a few) are all often explicitly or implicitly claimed to be superior stabilizers of nanoclusters. Relatively few of these putative stabilizers have ever been tested or ranked in any rigorous way,[7,12,13] however, except for those tested by the "five-criteria method" developed in 2002 for catalytically active nanoclusters and their stabilizers.[12,13] The stabilizers examined to date by the

* To whom correspondence should be addressed. E-mail: rfinke@lamar.colostate.edu.

(1) Schmid, G.; Chi, L. *Adv. Mater.* **1998**, *10*, 515.
(2) Schmid, G.; Baumle, M.; Geerkens, M.; Heim, I.; Osemann, C.; Sawitowski, T. *Chem. Soc. Rev.* **1999**, *28*, 179.

10.1021/cm062001h CCC: $40.75
Published on Web 03/12/2008

five-criteria method include halides,[31] polyoxo-polyanions,[12,13] hydrogenphosphate dianion,[32] citrate trianion,[12,13] ionic liquids,[33,34] polymers,[35] solvents,[36] and the weakly coordinating but surprisingly effective stabilizer BF_4^- in propylene carbonate solvent.[7,31,35,36] The interested reader is referred to these studies, efforts which provide the presently only available rankings of modern transition-metal nanocluster stabilizers in organic solvents. A review of the topic of "transition-metal nanocluster stabilization for catalysis: a critical review of ranking methods and stabilizers"[7] is also now available and is a model (the stabilizer−metal-lattice, surface-size-matching model or hypothesis[37]) for choosing between different stabilizers for selected transition-metal nanoclusters.

Despite these initial efforts, identifying and employing the truly best nanocluster stabilizer for the application at hand remains a largely unsolved problem.[7] For that matter, typically unknown are even which stabilizers allow for competent solution-phase stability, much less which stabilizers permit the isolation and full redissolution of the desired nanoclusters (e.g., all without bulk-metal formation in the case of transition-metal(0) nanoclusters). Such "bottleable" nanoclusters that can then be weighed out and used at any desired later time also require that the composition of the nanoclusters be firmly established, another surprisingly little accomplished goal, as Table 1 in a recent review[7] documents. Others have noted these same general problems, stating for transition-metal nanoclusters that "people in general cannot understand. . . which preparation method is the best among those proposed."[38]

The Problem of "What is the Best Nanocluster Stabilizer?". The research problem of "what is the best nanocluster stabilizer?" has several components: the first of which is the lack of a clear definition of stability for modern nanoclusters; the second issue is the lack of developed methods for quantitating nanocluster stability. A survey of the literature reveals that, at present, "stability" is often claimed on the basis of a (*ex situ*, solid state) transmission electron microscopy (TEM) image alone. "Good stability" is often claimed even if that image reveals agglomerated nanoclusters or even if bulk metal is in fact a major, albeit typically unreported,[7,39,40] product.

Examination of the extensive colloidal[41] literature reveals that (solution)[42] stability is arguably best defined by the ability of a chosen stabilizer to prevent agglomeration in solution. Notable in this context are the two literature methods, one 41 and the other 105 years old, for evaluating the stability (i.e., agglomeration tendency) of classical water-soluble colloids in the presence of gums, glues, starches, polymers, or other additives.[43,44] These old methods assay agglomeration visually but only qualitatively via the color change of red to purple as the Au colloids agglomerate. These old methods have been used to date only for water-soluble Au colloids, although they will probably also work for Ag and Cu because of the availability of a plasmon band in the visible region for Ag, Cu, and Au.[45,44] Hence, these plasmon-resonance-based methods[45] should, at least in principle, be extendable to modern Au, Ag, and Cu nanoclusters in organic solvents with a range of modern stabilizers and ligands, a goal

(3) Aiken, J. D., III; Finke, R. G. *J. Mol. Catal. A: Chem.* **1999**, *145*, 1.
(4) Finke, R. G. In *Metal Nanoparticles: Synthesis, Characterization, and Applications*; Feldheim, D. L., Foss, C. A., Jr., Eds.; Marcel Dekker: New York, 2002; Chapter 2, pp 17–54.
(5) Roucoux, A.; Schulz, J.; Patin, H. *Chem. Rev.* **2002**, *102*, 3757.
(6) Cushing, B. L.; Kolesnichenko, V. L.; O'Connor, C. J. *Chem. Rev.* **2004**, *104*, 3893.
(7) Ott, L. S.; Finke, R. G. *Coord. Chem. Rev.* **2007**, *251*, 1075–1110.
(8) Simon, U.; Schön, G.; Schmid, G. *Angew. Chem., Int. Ed.* **1993**, *32*, 250.
(9) Elghanian, R.; Storhoff, J. J.; Mucic, R. C.; Letsinger, R. L.; Mirkin, C. A. *Science* **1997**, *277*, 1078.
(10) Reetz, M. T.; Winter, M.; Dumpich, G.; Lohau, J.; Friedrichowski, S. *J. Am. Chem. Soc.* **1997**, *199*, 4539.
(11) Lin, Y.; Finke, R. G. *J. Am. Chem. Soc.* **1994**, *116*, 8335.
(12) Özkar, S.; Finke, R. G. *J. Am. Chem. Soc.* **2002**, *124*, 5796.
(13) Özkar, S.; Finke, R. G. *Langmuir* **2002**, *18*, 7653.
(14) Turkevich, J.; Kim, G. *Science* **1970**, *169*, 873.
(15) Chaudret, B.; Vidoni, O.; Philippot, K.; Amiens, C.; Balmes, O.; Malm, J.-O.; Bovin, J.-O.; Senocq, F.; Casanove, M.-J. *Angew. Chem., Int. Ed.* **1999**, *38*, 3736.
(16) Collier, P. J.; Iggo, J. A.; Whyman, R. *J. Mol. Catal. A: Chem.* **1999**, *146*, 149.
(17) Shiraishi, Y.; Arakawa, D.; Toshima, N. *Eur. Phys. J. E* **2002**, *8*, 377.
(18) Hirai, H.; Nakao, Y.; Toshima, N. *J. Macromol. Sci., Pure Appl. Chem.* **1979**, *13*, 727.
(19) Köhler, J. U.; Bradley, J. S. *Langmuir* **2000**, *14*, 2730.
(20) El-Sayed, M. A.; Narayanan, R. *J. Phys. Chem. B* **2004**, *108*, 8572.
(21) Crooks, R. M.; Zhao, M.; Sun, L.; Chechik, V.; Yeung, L. K. *Acc. Chem. Res.* **2001**, *34*, 181.
(22) Dagani, R. *Chem. Eng. News* **1999**, *77*, 33.
(23) Balogh, L.; Tomalia, D. A. *J. Am. Chem. Soc.* **1998**, *120*, 7355.
(24) Chauhan, B. P. S.; Rathore, J. S.; Chauhan, M.; Krawichz, A. *J. Am. Chem. Soc.* **2003**, *125*, 2876.
(25) Petit, C.; Lixon, P.; Pileni, M. P. *J. Phys. Chem.* **1993**, *97*, 12974.
(26) Dupont, J.; Fonseca, G. S.; Umpierre, A. P.; Fichtner, P. F. P.; Teixeira, S. R. *J. Am. Chem. Soc.* **2002**, *124*, 4228.
(27) Itoh, H.; Naka, K.; Chujo, Y. J. *Am. Chem. Soc.* **2004**, *126*, 3026.
(28) Cassol, C. C.; Umpierre, A. P.; Machado, G.; Wolke, S. I.; Dupont, J. *J. Am. Chem. Soc.* **2005**, *127*, 3298.
(29) Balasubramanian, R.; Beomseok, K.; Tripp, S. L.; Wang, X.; Lieberman, M.; Wei, A. *Langmuir* **2002**, *18*, 3676.
(30) Tripp, S. L.; Pusztay, S. V.; Ribbe, A. E.; Wei, A. *J. Am. Chem. Soc.* **2002**, *124*, 7914.
(31) Ott, L. S.; Cline, M. L.; Finke, R. G. *J. Nanosci. Nanotechnol.* **2007**, *7*, 2400–2007.
(32) Özkar, S.; Finke, R. G. *Langmuir* **2003**, *19*, 6247.
(33) Ott, L. S.; Campell, S.; Seddon, K. R.; Finke, R. G. *J. Am. Chem. Soc.* **2005**, *127*, 5758.
(34) Ott, L. S.; Campell, S.; Seddon, K. R.; Finke, R. G. E. *Inorg. Chem.* **2007**, *46*, 10335–10344.
(35) Ott, L. S.; Hornstein, B. J.; Finke, R. G. *Langmuir* **2006**, *22*, 9357.
(36) Ott, L. S.; Finke, R. G. *Inorg. Chem.* **2006**, *45*, 8382.
(37) Özkar, S.; Finke, R. G. *Coord. Chem. Rev.* **2004**, *248*, 135.
(38) Toshima, N.; Shiraishi, Y.; Teranishi, T.; Miyake, M.; Tominaga, T.; Watanabe, H.; Brijoux, W.; Bönnemann, H.; Schmid, G. *Appl. Organometal. Chem.* **2001**, *15*, 178.
(39) Besson, C.; Finney, E. E.; Finke, R. G. *J. Am. Chem. Soc.* **2005**, *127*, 8179.
(40) Besson, C.; Finney, E. E.; Finke, R. G. *Chem. Mater.* **2005**, *17*, 4925.
(41) Important distinctions between "nanoclusters" and "nanocolloids" are detailed in a previous contribution[4] (and, indeed, are experimentally apparent in the present work, such as the lack of a critical coagulation concentration for the polyxoanion-stabilized Ir(0) nanoclusters used in the present work). However, for the sake of simplicity, herein, we have chosen to distinguish the terms "nanocluster" from "colloid" or "nanocolloid" only where we felt it was important.
(42) In the solid-state, one useful practical definition of stability is the ability of a given stabilizer to prevent nanocluster agglomeration when the chosen nanoclusters are taken to dryness and then redissolved. Can they be fully redissolved without agglomeration as assayed by TEM (as well as by ≥1 other, independent method) and without bulk metal formation (as judged by the eye)? This definition, albeit qualitative, has proven to be one of the most stringent tests within the five-criteria method of ranking catalytically active nanoclusters.[12]
(43) Zsigmondy, R. *Z. Anal. Chem.* **1901**, 697.
(44) Thiele, H.; von Levern, H. S. *J. Colloid Interface Sci.* **1965**, *20*, 679.
(45) Creighton, J. A.; Eadon, D. G. *J. Chem. Soc., Faraday Trans.* **1991**, *87*, 3881.

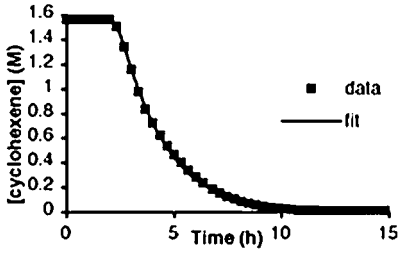

Figure 1. Characteristic, approaching step-function-shaped kinetic curve taken from our literature[39,40] with permission, which is well-fit by the four-step mechanism shown in Scheme 1. The system in this example is composed of (1,5-COD)$PtCl_2$ as the nanocluster precursor plus 2 equiv of Bu_3N and 2 equiv of proton sponge (1,8-bis(dimethylamino)naphthalene) in acetone solvent and with 1235 equiv of cyclohexene and at ca. 40 psig H_2.[39] The fit to the four-step mechanism in Scheme 1 (*vide infra*), shown as a line, is barely visible because the fit to the data is excellent. For clarity, only one of every eight data points collected is shown.

Scheme 1

$$A \xrightarrow{k_1} B$$
$$A+B \xrightarrow{k_2} 2B$$
$$2B \xrightarrow{k_3} C$$
$$B+C \xrightarrow{k_4} 1.5C$$

[a] A Is the organometallic precursor; B equals the nanoclusters; and C is agglomended metal.

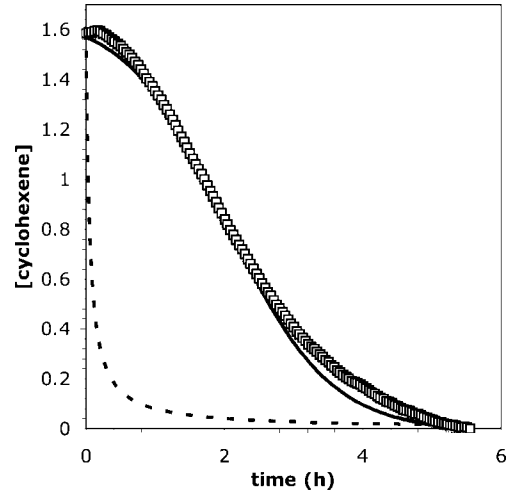

Figure 2. Thermal nanocluster agglomeration monitored by the concomitant cyclohexene hydrogenation at 40 °C beginning with isolated $Ir(0)_{\sim 900}$ nanoclusters. The cyclohexene hydrogenation data are shown as squares. The attempted "fit" using just the k_3 step of the mechanism shown in Scheme 1 is given as a dashed line, while the fit using both the k_3 and k_4 steps is given as a solid line. While both B and C are expected to be cyclohexene hydrogenation catalysts, the sigmoidal curve with its initially increasing rate implies that C is the faster catalyst consistent with recent findings.[39,40]

for future research as noted in the Summary. In short, proof of concept of a kinetic method that assays nanocluster stability based on measurement of the kinetics of nanocluster agglomeration in solution is an important research goal.[46] The ideal kinetic method or methods would be general, quantitative, and applicable to all metal nanoclusters in all solvents and stabilizers and all ligands of interest.

Highly relevant to addressing nanocluster stability in solution via agglomeration kinetic measurements are studies since 1997, which define the kinetics of formation,[39,40,47–52] and then agglomeration,[39,40,53] of modern transition-metal nanoclusters. More specifically, those prior kinetic and mechanistic studies allow us to propose, herein, that nanocluster solution stability is best, as well as most practically/experimentally, defined by the measurement of the two rate constants, k_3 and k_4, which define the only recently discovered two types of agglomeration processes, bimolecular and autocatalytic agglomerations, respectively.[39,40] Figure 1 provides an example of where the four-step mechanism for (in that case[39,40]) Pt(0) nanocluster nucleation (rate constant k_1), autocatalytic surface growth (k_2), bimolecular agglomeration (k_3), and autocatalytic agglomeration (k_4) are seen. Scheme 1 defines these four, k_1-k_4, rate constants in terms of the pseudo-elementary[48] steps that they represent.

To start, the measurement of k_3 and k_4 needs to be performed as a function of temperature and, ideally, also as a function of added, classical agglomerants of at least (classical) colloids, notably added salts, such as $[Bu_4N][BF_4]$, or basic ligands, pyridine being the classic example of a ligating agglomerant, again at least for classical colloids.[54] Salts induce agglomeration of classical colloids by causing the collapse of the multilayer that otherwise stabilizes anionically ligated, and thus Coulombic-repulsion (i.e., DLVO theory[7]) stabilized, colloids.[55] Added pyridine or other coordinating ligands are also known to induce agglomeration of classical colloids; the underlying mechanism is similar, the added pyridine or other neutral, coordinating ligand displaces surface-coordinated anions, thereby decreasing the anion-based Coulombic-repulsion stabilization,[7] again leading to agglomeration, at least of classical (i.e., not ultrastable) colloids.

Noteworthy, with respect to the prospect of measuring k_3 and k_4, it has only been since 2005, when the full four-step mechanism and its associated k_1-k_4 rate constants were first identified, that it has even been possible to correctly formulate, much less to perform, the studies that follow. That is, prior to the 2005 work, it was not even known that there are two rate constants, k_3 and k_4, that one needs to measure to quantitate agglomeration properly and completely. Moreover, the 2005 studies[39,40] also make clear that, at least ideally, one needs to aspire to measure both nucleation and growth (k_1 and k_2) as well as each of the two types of agglomeration (k_3 and k_4) in a single experiment. This would thereby ensure that the nanoclusters have been formed properly with good kinetic control (e.g., as indicated in many cases by a high k_2/k_1 ratio[12]) in the same experiment that their agglomeration, k_3 and k_4, is measured. This approach in turn avoids measuring the agglomeration of poorly formed, too highly polydisperse nano-

(46) Enüstün, B. V.; Turkevich, J. *J. Am. Chem. Soc.* **1963**, *85*, 3317.
(47) Lin, Y.; Finke, R. G. *Inorg. Chem.* **1994**, *33*, 4891.
(48) Watzky, M. A.; Finke, R. G. *J. Am. Chem. Soc.* **1997**, *119*, 10382.
(49) Widegren, J. A.; Aiken, J.D., III; Özkar, S.; Finke, R. G. *Chem. Mater.* **2001**, *13*, 312.
(50) Aiken, J. D., III; Finke, R. G. *Chem. Mater.* **1999**, *11*, 1035.
(51) Hornstein, B. J.; Aiken, J. D., III; Finke, R. G. *Inorg. Chem.* **2002**, *41*, 1625.
(52) Widegren, J. A.; Finke, R. G. *Inorg. Chem.* **2002**, *41*, 1558.
(53) Hornstein, B. J.; Finke, R. G. *Chem. Mater.* **2004**, *16*, 139.
(54) Pyridine as a classic agglomerant of (classical) colloids: (a) Weitz, D. A.; Huang, J. S.; Lin, M. Y.; Sung, J. *Phys. Rev. Lett.* **1985**, *54*, 1416. (b) Blatchford, C. G.; Campbell, J. R.; Creighton, J. A. *Surf. Sci.* **1982**, *120*, 435.
(55) Evans, D. F.; Wennerström, H. *The Colloidal Domain*, 2nd ed.; Wiley-VCH: New York, 1999.

clusters, a measure that in turn avoids a version of the "garbage in, garbage out" syndrome. Hence, efforts attempting to measure k_1-k_4 simultaneously will, therefore and necessarily, be addressed in what follows, such studies, albeit less successful, having been the target of substantial effort over the 5 years since we first started the studies reported herein. An alternative and as it turns out more successful approach is to measure just k_3 and k_4 of pre-isolated, well-characterized nanoclusters that are near monodisperse (i.e., of $\leq \pm 15\%$ size dispersion[3]). The obvious drawback to this approach is that one is, in turn, limited to stability studies of only the more (if not the most) stable, isolable nanoclusters.

Herein, we report our efforts directed at the specific goal of measuring the k_3 and k_4 agglomeration kinetics rate constants for prototype, preformed $Ir(0)_{\sim 900}$ nanoclusters. We have been able to measure both k_3 and k_4 as well as their temperature dependence of these preformed nanoclusters. The resulting, previously unavailable $\Delta H^{\ddagger}$ and $\Delta S^{\ddagger}$ for each of two nanocluster agglomeration steps proved especially interesting and informative, suggesting that the k_3 type of agglomeration may be associatively activated, while the k_4 type appears to be dissociatively activated. We also attempted agglomeration of preformed $Ir(0)_{\sim 900}$ nanoclusters with $[Bu_4N][BF_4]$ but found they are too stable to be agglomerated by at least this salt. Reported primarily in the Supporting Information are extensive studies attempting to simultaneously measure the kinetics and k_1-k_4 rate constants of nucleation, growth, and the two types of agglomeration: (a) in situ generated $P_2W_{15}Nb_3O_{62}^{9-}$-stabilized $Ir(0)_n$ nanoclusters in the presence of added salt, $[Bu_4N][BF_4]$, or pyridine as agglomerating agents and (b) in situ generated $Ir(0)_n$ nanoclusters separately stabilized by four different anions in both acetone and propylene carbonate solvent with added pyridine as the agglomerant. The Summary discusses the eight insights generated by the present work as well as some goals for future research in the area of assaying nanocluster stability via kinetic measurements of agglomeration.

Results and Discussion

Quantitation of Nanocluster Agglomeration as a Function of Temperature using Preformed, Isolated, and then Redispersed $P_2W_{15}Nb_3O_{62}^{9-}$-Stabilized $Ir(0)_{\sim 900}$ Nanoclusters. To start, we studied the agglomeration of preformed, isolated $P_2W_{15}Nb_3O_{62}^{9-}$-stabilized $Ir(0)_{\sim 900}$ nanoclusters as a function of the temperature (i.e., and in the absence of any other agglomerating agent) and using the cyclohexene reporter reaction method.[39,40,48] A representative cyclohexene hydrogenation (i.e., cyclohexene loss) curve at 40 °C is shown as Figure 2. To investigate the mechanism, two fits using the reactions shown in Scheme 1 are also shown: the attempted fit using only the k_3, $B + B \rightarrow C$ agglomeration step is woefully inadequate for the observed data, Figure 2. Conversely, the data are reasonably well-fit when an autocatalytic step is added (i.e., when using both the k_3 and k_4 steps shown in Scheme 1); that is, it is clear that both a k_3 step and an autocatalytic, k_4 step are necessary to fit the data.

In important control experiments, we showed that k_3 and k_4 are not functions of the [cyclohexene], as expected when the cyclohexene reporter reaction is working without complications.[39,40,48,49] Three reactions at 50 °C were performed, beginning with preformed nanoclusters and 0.25 mL (experiment 1), 0.5 mL (experiment 2), and 1.0 mL (experiment 3) cyclohexene. Although the observed k_3 and k_4 rate constants did exhibit some scatter, there is no obvious trend in rate constants as a function of the olefin concentration.[56] Hence, it appears that the cyclohexene reporter reaction[39,40,48] is performing properly in this case. Provided in the Supporting Information for the interested reader are the specific equations that show how the loss of cyclohexene (Figure 1) is connected to the loss of B or formation of C by the pseudo-elementary step treatment.

Verification of Agglomeration by TEM. Because we only disprove in science in general and mechanism in particular,[57] because verification of the reaction stoichiometry is the first step in reliable mechanism, and also because something such as a "$A \rightarrow B$, $A + B \rightarrow 2B$" mechanism could masquerade as the proposed $B + B \rightarrow C$ and then $B + C \rightarrow 1.5C$ mechanism (e.g., where the $A \rightarrow B$ conversion could conceivably be some type of activation process needed for the hydrogenation reporter reaction), it is crucial to verify that agglomeration has in fact taken place. The needed TEM studies are shown in Figure 3 and confirm that agglomeration has occurred. In addition, from synthesis, we know that we are starting with preformed nanoclusters, by definition "B", in the present studies, not the nanocluster precursor[39,40] A.

The agglomeration experiments also provide the first experimental glimpse on the sizes of B and C, at least for the present $Ir(0)_n$ nanoclusters and the specific conditions employed. Because isolated $Ir(0)_{\sim 900}$ nanoclusters are (again by definition) species B in the present case (i.e., by the fact that the kinetic fits are to $B + B \rightarrow C$ and $B + C \rightarrow 1.5C$), it follows that C must be particles at least twice as large on average as 900 metal atoms (i.e., $\approx$1800 or $\approx$2000 after rounding up). That is, C must be $\geq Ir(0)_{\sim 2000}$ in the present case relative to starting $B \approx Ir(0)_{\sim 900}$. The TEM images in Figure 3 confirm this expectation: the starting $Ir(0)_{\sim 900}$ nanoclusters[58] have agglomerated to roughly 2.2 larger size on average, 3.8 ± 0.6 nm $Ir(0)_{\sim 2000}$, after the cyclohexene hydrogenation catalysis at 50 °C. There are also some even larger, 6–7 nm agglomerates, C, visible in Figure 3.

Measurement of k_3 and k_4 as a Function of the Temperature. Pleasingly, the agglomeration rate constants k_3 and k_4 also proved measurable as a function of the temperature (from 10 to 50 °C; Figures S1−S5 of the Supporting Information provide the raw kinetic data and associated fits). The key results are summarized in Table 1.

The data in Table 1 confirm that both k_3 and k_4 increase with the temperature as expected. The results are significant even if they are for the specific case of nanoclusters simultaneously undergoing hydrogenation catalysis: they represent the first experimental, quantitative measurement

(56) The observed rate constants from the experiments with 0.25, 0.5, and 1.0 mL cyclohexene, respectively, are $k_3 = 0.13\ M^{-1}\ h^{-1}$, $k_4 = 0.56\ M^{-1}\ h^{-1}$; $k_3 = 0.028\ M^{-1}\ h^{-1}$, $k_4 = 1.9\ M^{-1}\ h^{-1}$; $k_1 = 0.019\ M^{-1}\ h^{-1}$, $k_4 = 0.22\ M^{-1}\ h^{-1}$. The scatter in these data reveal the relative large error in any single k_3 plus k_4 kinetic run.

(57) (a) Platt, J. R. *Science* **1964**, *146*, 347. (b) Chamberlin, T. C. *J. Geol.* **1897**, *5*, 837 (yes, the year, 1897, of this more than 100 year old, classic paper is correct, a paper that is a wonderful reading along with Platt's classic paper)[57a]

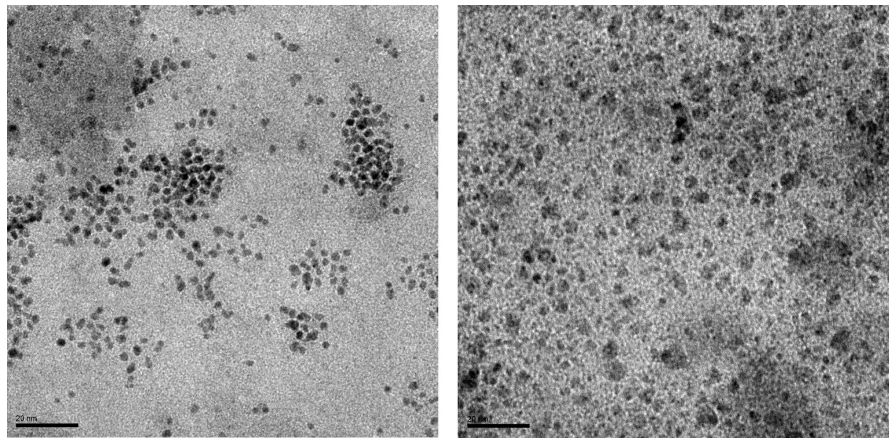

Figure 3. TEM micrographs of the isolated Ir(0) nanoclusters as prepared (left) and after agglomeration and concomitant cyclohexene hydrogenation catalysis at 50 °C (right). The scale bar is 20 nm in each micrograph. The as-prepared nanoclusters are smaller, 2.7 ± 0.4 nm (i.e., a bit smaller on average than the nanoclusters prepared in our earlier study[67]), and show a ±15% size distribution, while the nanoclusters after catalysis (plus agglomeration) are larger, 4.0 ± 1.5 nm, and show a broader, ±38% size distribution. The results are consistent with and supportive of the proposed agglomeration steps, B + B → C and B + C → 1.5C.

Table 1. Rate Constants k_3 and k_4 for $P_2W_{15}Nb_3O_{62}^{9-}$-Stabilized Nanoclusters from 10 to 50 °C in Propylene Carbonate Solvent[59] and under Hydrogenation Conditions, Fit with C as the Cyclohexne Hydrogenation Catalyst[a]

temperature (°C)	k_3 (h^{-1} M^{-1})	k_4 (h^{-1} M^{-1})
10	0.0074(7)	0.053(1)
20	0.0078(7)	0.105(6)
30	0.015(1)	0.60(3)
40	0.025(2)	1.71(7)
50	0.028(1)	1.9(2)

[a] Each rate constant shown is the result of ≥5 fitting trials.

of nanocluster agglomeration from isolated, bottleable nanoclusters, including the first measurement of both of the rate constants defining the two types of agglomeration represented by k_3 and k_4 (again for Ir(0) nanoclusters undergoing hydrogenation catalysis).

Note that it is in some ways surprising that bottleable nanoclusters with the superior, present "gold standard" polyanionic, $P_2W_{15}Nb_3O_{62}^{9-}$ polyoxoanion stabilizer can be agglomerated at such mild temperatures. It follows that the presence of the cyclohexene and/or hydrogen, and the associated hydrogenation catalysis is very likely a component of the agglomeration process and, therefore, the resultant k_3 and k_4 being measured in this initial test case.

The results permit the calculation of the previously unavailable activation parameters for the k_3 and k_4 processes using the Eyring equation:[60] $\Delta H_3^{\ddagger}$=6.2(3) kcal/mol[61] and $\Delta S_3^{\ddagger} = -46(2)$ eu and $\Delta H_4^{\ddagger} = 18(1)$ kcal/mol and $\Delta S_4^{\ddagger} = -2.5(2)$ eu (standard state = 1 M). Figure 4 presents the Eyring plots and associated error bars. The precision of the data is a bit lower (and hence the associated 2σ error bars are a bit higher) than ideally desired (Figure 4), but the data still adequately define the activation parameters for the purposes of this first study. Notably, the specific values of the activation parameters suggest insight into the (two different) mechanisms of agglomeration for the k_3 and k_4 steps:[62] the $\Delta H_3^{\ddagger}$ and $\Delta S_3^{\ddagger}$ values suggest (but, of course, cannot unequivocally demonstrate by themselves) that the k_3, B + B → C step proceeds via primarily an associatively activated mechanism, that is, one in which the nanoclusters agglomerate (we infer) before coordinated $P_2W_{15}Nb_3O_{62}^{9-}$ and/or solvent ligands dissociates from the surface. Conversely, the magnitude of $\Delta H_4^{\ddagger}$ and $\Delta S_4^{\ddagger}$ suggest (but, again, cannot unequivocally prove) that the k_4, B + C → 1.5C step proceeds via a dissociatively activated mechanism, involving (we infer) $P_2W_{15}Nb_3O_{62}^{9-}$ and/or solvent, leaving the nanocluster surface before agglomeration occurs. Again, these activation parameters refer to the specific conditions in which the Ir(0) nanoclusters are in the presence of cyclohexene and H_2 and undergo concomitant olefin hydrogenation.

Also noteworthy here are these activation parameters, and the agglomeration mechanisms that they suggest are consistent with the hypothesis[39,40] that metal–ligand bond energies can be up to 2-fold stronger in nanoparticles (B, leading to a associative mechanism) versus those in the larger C particles that presumably begin to look like bulk metal[39,40] (leading to a dissociative mechanism). This statement follows because one would expect the species (B versus C) with the lowest surface-metal−ligand bond dissociation

(58) The 2.7 ± 0.4 nm Ir(0) nanoclusters used in the present study and which correspond to an average size of $Ir(0)_{\sim 900}$ are on average a bit smaller than those estimated as 3.8 ± 0.6 nm ($Ir(0)_{\sim 2000}$) in our prior work, in which we were able to count only 120 nanoclusters. The agglomerated nanoclusters herein are 4.0 ± 1.5 nm, corresponding to an average size of $Ir(0)_{\sim 2000}$, which in turn is ca. 2.2 times as large, on average, versus the initial $Ir(0)_{\sim 900}$nanoclusters.

(59) The reader may wonder if the change in solvent from that employed in many of our earlier studies, acetone, to propylene carbonate, can contribute to a change in mechanism. The data in Table S1 of the Supporting Information demonstrate that the answer is no, at least in the present case and under the specific conditions used in the present studies.

(60) Wilkins, R. G. *Kinetics and Mechanism of Reactions of Transition-Metal Complexes*; VCH Publishers, Inc.: New York, 1991; pp 88–89.

(61) The $\Delta H_\eta^{\ddagger}$ (activation enthalpy for viscous flow) is $\Delta H_\eta^{\ddagger} \cong 2.3$ kcal/mol for propylene carbonate (For the viscosity versus temperature data used to calculate $\Delta H_\eta^{\ddagger}$, see (a) Barthel, J.; Neueder, R.; Roch, H. *J. Chem. Eng. Data* **2000**, *45*, 1007. For the method used to calculate $\Delta H_\eta^{\ddagger}$, see footnote 31 in Hay, B. P.; Finke, R. G. *J. Am. Chem. Soc.* **1987**, *109*, 8012). The $\Delta H_3^{\ddagger} = 6.2(3)$ kcal/mol is, therefore, larger than just the barrier to diffusion in propylene carbonate, so that other factors besides diffusion must be introducing a barrier into the B + B → C agglomeration process.

(62) Espenson, J. H. *Chemical Kinetics and Reaction Mechanisms*, McGraw-Hill: New York, 1995; Chapter 7.

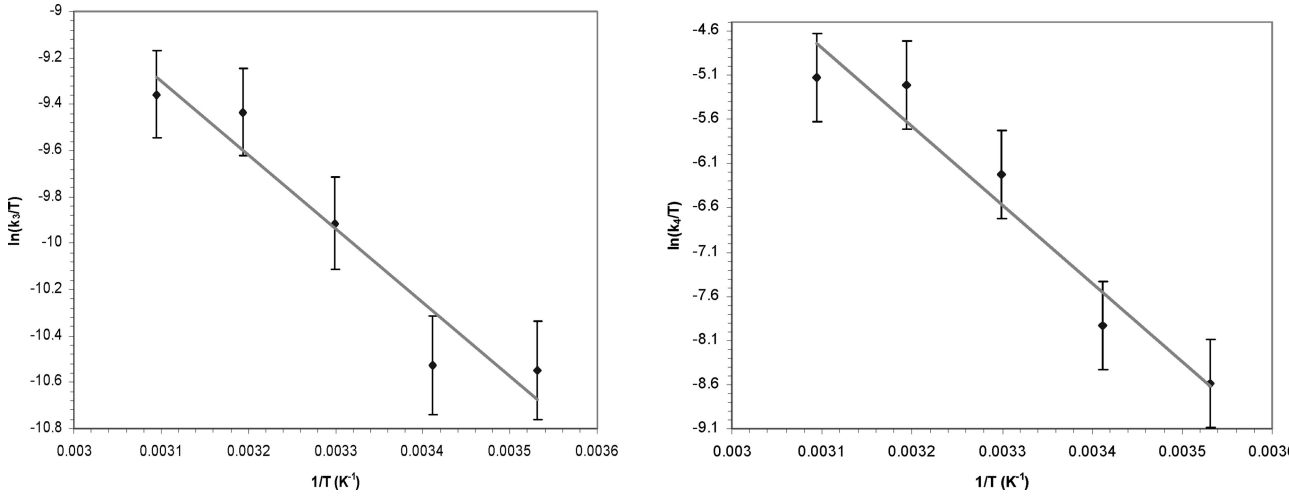

Figure 4. Eyring plots for k_3 (left) and k_4 (right). The error bars shown are given at 2σ.

energy to have the dissociative mechanism; as predicted,[39,40] it is the k_4 step involving C. The interested reader is referred to footnote 63, the Supporting Information, as well as to the discussion elsewhere[39,40] for more on the topic of metal particle size-dependent bond energies and surface coverages.

It occurred to us towards the end of our studies that we do have one set of temperature-dependent k_1, k_2, k_3 and k_4 rate constants from the reduction of Pt(1,5-COD)Cl_2 under H_2 that could serve as a control of sorts to see if those computed activation parameters supported, or contrasted, the above findings for $Ir(0)_n$ nanoclusters. Unfortunately, the low precision of that data—always a problem when one is searching the 5-dimensional space consisting of 4 rate constants plus a residual[39,40]—is such that no definitive conclusions could be drawn, although the *speculative implications* from those imprecise activation parameters are that k_3 and k_4 may *not* be associatively and dissociatively activated, respectively, at least for this different, $Pt(0)_n$ metal plus completely different (Cl^-) stabilizer system. Those raw activation parameter data plus additional discussion are summarized in the Supporting Information for the interested reader.

Attempted Initiation of Nanocluster Agglomeration by Added [Bu$_4$N][BF$_4$] and Using Preformed, Isolated, and then Redispersed $P_2W_{15}Nb_3O_{62}^{9-}$-Stabilized Ir(0)$_{\sim 900}$ Nanoclusters: Confirmation of the Stability of $P_2W_{15}Nb_3O_{62}^{9-}$ Polyoxoanion-Stabilized Ir(0) Nanoclusters. The literature teaches that one of the classic methods of agglomerating anionically ligated, Coulombic-repulsion-stabilized colloidal solutions is with added salts; they collapse the double (really multi) layer, leading to physically closer nanoclusters and, hence, increased agglomeration rates.[7] Hence, we attempted to induce agglomeration of the $P_2W_{15}Nb_3O_{62}^{9-}$-stabilized, pre-isolated, and redispersed $Ir(0)_{\sim 900}$ nanoclusters with 0–500 added equivalents of [Bu$_4$N][BF$_4$] at 40 °C.

The data in Table 2 below reveal that even 500 equiv of added [Bu$_4$N][BF$_4$] does not change the k_3 rate constant. Additionally, the k_4 rate constant remains unchanged within a factor of 2.5 even as the number of equivalents of [Bu$_4$N][BF$_4$] changes by a factor of 500. That is, both k_3 and k_4 remain constant within what is probably the true experimental error of the data.[56] Hence, preformed $P_2W_{15}Nb_3O_{62}^{9-}$-stabilized $Ir(0)_{\sim 900}$ nanoclusters are apparently too stable to induce additional agglomeration using high salt concentrations of at least [Bu$_4$N][BF$_4$].

Table 2. Rate Constants k_3 and k_4 for the B + B → C and B + C → 1.5C Steps, Respectively, with Added [Bu$_4$N][BF$_4$] at 40 °C[a]

[Bu$_4$N][BF$_4$]	k_3 (h^{-1} M^{-1})	k_4 (h^{-1} M^{-1})
0 equiv	35(3)	$2.4(1) \times 10^3$
100 equiv	36(3)	$1.09(3) \times 10^3$
200 equiv	39.8(3)	$2.12(1) \times 10^3$
500 equiv	49(1)	$0.94(4) \times 10^3$
average	41(8)	$1.7(7) \times 10^3$

[a] The rate constant k_3 does not change systematically beyond what is probably the true experimental error; the k_4 rate constant remains unchanged within a factor of 2.5 even though the number of equivalents of [Bu$_4$N][BF$_4$] changes by a factor of 500. In short, neither the k_3 nor k_4 values change beyond experimental error even after 500 equiv of [Bu$_4$N][BF$_4$] has been added.

We considered pursing an extensive study of other salts, and this remains a possible avenue of future investigation. However, upon reflection, we decided at this time not to study other salts as possibly better agglomerants because the inability of [Bu$_4$N][BF$_4$] and probably other, at least monovalent anion and cation salts to induce agglomeration of $P_2W_{15}Nb_3O_{62}^{9-}$-stabilized $Ir(0)_{\sim 900}$ nanoclusters is not surprising to us. It is an interesting observation, however, one relevant to what is and is not know about the stabilization of modern transition-metal nanoclusters. Specifically, the lack of any sizable effect of even 500 equiv of added [Bu$_4$N][BF$_4$] nicely confirms the high, anionic stabilization by the $P_2W_{15}Nb_3O_{62}^{9-}$ polyoxoanion as measured by the five-criteria method.[7,12] This finding that $P_2W_{15}Nb_3O_{62}^{9-}$-stabilized Ir(0) nanoclusters are too stable to be easily agglomerated by at least [Bu$_4$N][BF$_4$] is also fully consistent with an earlier piece of evidence indicating the high stability of $P_2W_{15}Nb_3O_{62}^{9-}$-stabilized Ir(0) nanoclusters[12] and their difference in comparison to classical colloids:[7] these specific Ir(0) nanoclusters can be taken to dryness and redissolved without detectable agglomeration by TEM. In the language of classical colloids, they lack a so-called "critical coagula-

tion constant" (ccc), typically measured by the amount of salt it takes to cause agglomeration/coagulation of the colloid being tested. This lack of a ccc plus the inability to induce agglomeration of $P_2W_{15}Nb_3O_{62}^{9-}$-stabilized Ir(0) nanoclusters by even 500 equiv of added $[Bu_4N][BF_4]$ highlight both the stability of these *electrosterically*[7] *stabilized* nanoclusters as well as their distinction from classical colloids in aqueous solution that do show a ccc.

Attempts to Measure k_1-k_4 for Either *in Situ* Generated $Ir(0)_n$ Nanoclusters or Pre-isolated $Ir(0)_{\sim 900}$ Nanoclusters with Added Pyridine as the Agglomerant. We performed three general types of studies attempting to measure k_1-k_4 simultaneously under conditions that favor agglomeration, specifically (i) studies starting with the premade organometallic precursor $(Bu_4N)_5Na_3[(1,5\text{-COD})\text{-}Ir\cdot P_2W_{15}Nb_3O_{62}]$ placed in either acetone or propylene carbonate solvent with 0–75 equiv added pyridine, (ii) studies preparing the nanocluster precursor *in situ* starting with the organometallic precursor $[(1,5\text{-COD})Ir(CH_3CN)_2][BF_4]$ and the $[Bu_4N]^+$ salts of $P_2W_{15}Nb_3O_{62}^{9-}$, HPO_4^{2-}, Cl^-, and BF_4^- in either acetone or propylene carbonate solvent with 0–10 equiv added pyridine, and (iii) studies investigating if we could measure the two agglomeration rate constants separately by adding pyridine to preformed $P_2W_{15}Nb_3O_{62}^{9-}$-stabilized $Ir(0)_{\sim 900}$ nanoclusters in propylene carbonate solvent.

Despite a considerable amount of effort on these specific goals on and off over a period spanning 5 years, we were unable to find a set of conditions (solvent, nanocluster-stabilizing anion, and amount of pyridine agglomerant) where agglomeration was measurable and the cyclohexene reporter reaction could be unequivocally demonstrated to be properly amplifying the kinetics of nanocluster formation (as verified by a zero-order dependence on the cyclohexene concentration;[48] more discussion of this and the cyclohexene reporter reaction are provided in the Supporting Information for the interested reader). In general, added pyridine agglomerant appears to bind to the nanocluster surface as one would expect; added pyridine also introduces a non-zero-order dependence on the [cyclohexene], again as one might expect because the olefin and pyridine are in competition for surface active sites. Overall, one cannot be absolutely sure that the cyclohexene hydrogenation catalytic reporter reaction is working properly by the previously successful, simple control of testing for a zero-order, $[\text{cyclohexene}]^0$ dependence.[48] The experimental details and results of these experiments are reported in detail in the Supporting Information for the interested reader.

The results are still useful, however, because they indicate that an important, future research challenge is the development of additional physical methods to obtain the nanocluster agglomeration k_3 and k_4 rate constants. As for the possible physical methods for monitoring agglomeration that appear most promising at present, the following methods merit scrutiny in our opinion: (a) calorimetry, first and foremost, because it is possibly a more general method, (b) UV–vis spectroscopy (i.e., for metals with a plasmon in the visible region, Ag, Au, and Cu),[45] and (c) XAFS and/or SAXS/WAXS. One can also imagine using (d) nanoclusters with a specific label or optical probe that is either released or changes it spectrum following agglomeration. Each of these methods is under further, collaborative experimental scrutiny.[64]

Summary

The main findings herein then are as follows:

• An experimental way to quantitate nanocluster stability and thereby rank stabilizers was developed, specifically the measurement of the k_3 and k_4 rate constants for, respectively, bimolecular and autocatalytic agglomeration. This in turn provides a modern, working definition of nanocluster stability for the first time in terms of relative k_3 and k_4 rate constants for different stabilizers (i.e., under conditions where the other variables of the chosen system are carefully controlled).

• The k_3 and k_4 rate constants for the temperature-induced agglomeration of $Ir(0)_{\sim 900}$ nanoclusters concomitantly undergoing cyclohexene hydrogenation were successfully quantitated. We note here, however, that we consider these initial rate constants and their temperature dependence (*vide infra*) *as just initial values that need to* be *checked by other, more direct physical methods* to ensure that they or perhaps their updated versions can become benchmarks for others studies. In addition, studies of nanocluster agglomeration without cyclohexene and H_2 present are a needed next step as is independent verification by other physical methods of the B + B → C and B + C → 1.5C agglomeration mechanism.

• The rate constants versus the temperature were provided that, in turn, (i) yield the activation parameters for the two agglomeration steps, $\Delta H_3^{\ddagger} = 6.2(3)$ kcal/mol and $\Delta S_3^{\ddagger} = -46(2)$ eu and $\Delta H_4^{\ddagger} = 18(1)$ kcal/mol and $\Delta S_4^{\ddagger} = -2.5(2)$ eu (standard state = 1 M) under the specific conditions examined, (ii) provide evidence suggesting that the mechanisms of the agglomeration steps are different and, apparently, associative, for the k_3 step but dissociative for the k_4 step, and (iii) thereby offer further support for the fact that there really are two kinds of agglomeration that differ physically, as elucidated only recently.[39,40]

• The first experimental glimpse was provided into the sizes of C $(Ir(0)_{\geq 2000})$ versus starting B $(Ir(0)_{\sim 900})$, and those results were supported by TEM studies.

• The classical colloid agglomerant of added salt was found to be ineffective in inducing the agglomeration of highly

(63) Intriguing mechanistic questions are opened up by these findings. One is whether an associative mechanism occurs via bridging ligands that might, conceivably, bind the two metal particles, thereby giving the surface ligands more time to move, leaving larger bare-metal spots that are presumably key to the metal−metal bond formation process that leads to larger metal aggregates. Alternatively, another interesting question is if there are sufficient bare-metal spots on the surface of the nanocluster to support a direct, associative agglomeration, or is a mere single, bare-metal atom sufficient to initiate agglomeration? A third important question is how much the olefin (i.e., the cyclohexene used in the reporter reaction) is influencing the observed activation parameters, something that should be addressable by examining other olefins or, better, repeats of the present studies by other methods without and then with cyclohexene, H_2, and then both cyclohexene and H_2present.

(64) W. E. Buhro and R. G. Finke research groups. Collaborative studies in progress.

electrosterically[7] stabilized $P_2W_{15}Nb_3O_{62}^{9-}$-ligated $Ir(0)_{\sim 900}$ nanoclusters and at least for the specific monovalent salt, $[Bu_4N][BF_4]$. The results are important, however, in confirming the novelty and high level of coordinated-anion-imparted stability present in $P_2W_{15}Nb_3O_{62}^{9-}$ polyoxoanion-stabilized nanoclusters.[12]

• The results open the door for quantitatively ranking what has been termed the "dizzying variety"[6] of nanocluster stabilizers in the literature, with the significant caveat here being that only nanoclusters that are stable enough to be isolated and redissolved without the formation of bulk metal can be examined using the methods developed in the present work. Dependent upon one's point of view, this caveat is either a serious limitation or a greatly simplifying approach (i.e., limiting nanocluster stabilizers to those few that allow for the isolation of the nanoclusters without agglomeration and thus are worthy of such k_3 and k_4 kinetic measurements).

• The present work also therefore makes it clear that further studies, by other physical methods, quantitating the rate constants of nanocluster agglomeration are badly needed. In particular, the need is for methods that will allow all four rate constants k_1-k_4 to be measured (i.e., when the four-step mechanism can be shown to be operative) under a variety of conditions for a variety of nanocluster precursors, added stabilizers, solvents, and classical as well as to-be-developed agglomerants. Our hopefully somewhat educated guess at present is that most valuable might be (i) calorimetry, (ii) UV–vis spectroscopy (i.e., for metals with a plasmon absorbance, such as Ag, Au, and Cu),[45] (iii) XAFS and/or SAXS/WAXS, and (iv) possibly methods that employ nanoclusters specifically labeled/tagged with groups that change their response upon agglomeration. Each of these methods is under further, collaborative consideration and, where appropriate, experimental scrutiny.[64]

• One final point worth mentioning is that, because of the bimolecular $B + B \rightarrow C$ and $B + C \rightarrow 1.5C$ nature of the agglomeration steps, low concentrations of poorly stabilized and thus often highly catalytically active nanoclusters can (a) have long catalytic lifetimes and (b) can, therefore, do considerable "hidden" catalysis. These points are little appreciated but we suspect probably profound for catalysis (see elsewhere for a further discussion of this point[7]).

Experimental Section

Materials. All commercially obtained reagents were used as received unless otherwise noted. All solvents and compounds were stored in a drybox prior to use. Propylene carbonate (Aldrich, 99.7%) was evacuated under vacuum for at least 4 h and stored over activated 4 Å molecular sieves. Acetone (Burdick and Jackson, 99.9+% by GC) was purged with argon for a minimum of 20 min. Cyclohexene (Aldrich, 99%) was freshly distilled over Na metal under argon. CD_2Cl_2 and CD_3CN (Cambridge Isotope Laboratories, 99.9%) were purchased in prescored 1 g amber glass vials. The polyoxoanion $[Bu_4N]_9[P_2W_{15}Nb_3O_{62}]$ was prepared according to our most recent literature procedure.[65] The purity of the polyoxoanion was confirmed by ^{31}P NMR (CD_3CN δ: −6.5, −13.6 relative to 85% H_3PO_4, with small impurity peaks at δ −8.7 and −13.2). $[Bu_4N]_5Na_3[(1,5\text{-COD})Ir\cdot P_2W_{15}Nb_3O_{62}]$ was prepared using the literature procedure, with the exception that crystalline $[(1,5\text{-COD})Ir(CH_3CN)_2][BF_4]$ was used as the Ir source.[56] Proton sponge (1,8-bis(dimethylamino)naphthalene, Aldrich, 99%) and $[Bu_4N][BF_4]$ (Aldrich, 99%) were used as received.

Instrumentation. Nuclear magnetic resonance (NMR) spectra were obtained at 22 °C on a Varian Inova 300 MHz instrument. Spectral parameters for ^1H NMR include: tip angle, 38.9°; acquisition time, 2.372 s; relaxation delay, 1.000 s; and sweep width, 6000.6 Hz. Spectral parameters for ^{31}P NMR include: tip angle, 88.2°; acquisition time, 1.600 s; and sweep width, 10 000.0 Hz.

Hydrogenation Apparatus and the Catalytic Reporter Reaction. Hydrogenation experiments used to monitor the conversion of B into C (see the Supporting Information for further details on the catalytic reporter reaction method) were carried out in a previously fully described[11,48,50] apparatus designed to continuously monitor pressure loss. The H_2 used for hydrogenations is purchased in >99.9% purity (General Air) and passed through H_2O and O_2 scavenging traps (Trigon Technologies). This apparatus consists of a Fisher-Porter (F-P) bottle, which connects via Swagelok Quick-Connects to both a H_2 line and an Omega PX621 pressure transducer. The pressure transducer is interfaced with a PC by means of an Omega D1131 5V A/D converter with a RS-232 connection. The pressure uptake data were collected using LabView 7.1. These hydrogen uptake curves were converted to cyclohexene consumption curves using the known 1:1 H_2/cyclohexene stoichiometry.[49] During the hydrogenation reactions, the F-P bottle was immersed in a 500 mL jacketed reaction flask (Ace Glass, Inc.). The flask was filled with dimethyl silicon fluid (Thomas Scientific), and the temperature of the flask was regulated with a thermostatted recirculating water bath (VWR).

Experimental evidence is available elsewhere[40] showing that the catalytic reporter reaction accurately reports the kinetics of, for example, the four-step mechanism illustrated, in Figure 1 for the case of Pt nanoclusters, the case where the four-step mechanism was first discovered.[39,40] More specifically, the catalytic reporter reaction method (i.e., the H_2 uptake and cyclohexene loss kinetics) and the four-step mechanism were verified by independent, albeit far less precise, NMR and GLC kinetic methods (see p 4932 and Figure 6 elsewhere).[40]

Nanocluster Formation from $[Bu_4N]_5Na_3[(1,5\text{-COD})Ir\cdot P_2W_{15}Nb_3O_{62}]$. For this reference nanocluster formation reaction, one known to have no measurable agglomeration rate (i.e., the nanoclusters are highly stabilized[7,12,13]), $[Bu_4N]_5Na_3[(1,5\text{-COD})Ir\cdot P_2W_{15}Nb_3O_{62}]$ (20.0 mg, 3.6 μmol) was weighed into a predried 2 g glass vial in the drybox. Next, proton sponge (0.8 mg, 3.6 μmol) was added to the vial. Then, acetone (e.g., for Figure 1) or propylene carbonate (2.5 mL) was added with a 1.0 mL gastight syringe, yielding a clear, brilliant-yellow solution. The solution was agitated with a polyethylene pipet until it was homogeneous and then transferred with the same pipet to a new borosilicate culture tube (22 × 175 mm) with a new $^5/_8 \times {}^5/_{16}$ in. Teflon-coated, octagon-shaped spin bar. Freshly distilled cyclohexene (0.5 mL) was added to the culture tube with a 1.0 mL gastight syringe. The culture tube was placed in the F-P bottle, which was sealed, brought out of the drybox, and attached to the H_2 line via its Quick-Connects. To begin each reaction, the F-P bottle was purged 13 times with H_2 (40 ± 1 psig, 15 s/purge). At 5 min after the first purge, the pressure was set at 40 ± 1 psig, $t = 0$ was noted, and pressure versus time data

(65) Hornstein, B. J.; Finke, R. G. *Inorg. Chem.* **2002**, *41*, 2720.
(66) Pohl, M.; Lyon, D. K.; Mizuno, N.; Nomiya, K.; Finke, R. G. *Inorg. Chem.* **1995**, *34*, 1413.
(67) Hornstein, B. J.; Finke, R. G. *Chem. Mater.* **2003**, *15*, 899.
(68) (a) Kuzmic, P. *Anal. Biochem.* **1996**, *237*, 260. (b) http://uwmml.pharmacy.wisc.edu.

were collected at 2.5 min intervals. Table S1 of the Supporting Information shows the five criteria for $[Bu_4N]_5Na_3[(1,5\text{-COD})Ir{\cdot}P_2W_{15}Nb_3O_{62}]$ reduction under H_2 in the presence of proton sponge in both acetone and propylene carbonate solvent. The essence of the data for this experiment in Table S1 of the Supporting Information is that near monodisperse, isolable, and redissolvable nanoclusters are formed in both solvents with kinetics of formation that are well-fit by the two-step mechanism for nanocluster formation[48] (i.e., thus with no detectable agglomeration k_3 or k_4).

Nanocluster Agglomeration Reactions Beginning with Isolated $Ir(0)_{\sim 900}$ Nanoclusters at Varying Temperatures. $Ir(0)_{\sim 900}$ nanoclusters (with the literature average molecular formula of the slightly larger $[(n\text{-}C_4H_9)_4N]_{\sim 1000}Na_{\sim 5000}Ir_{\sim 2000}(P_4W_{30}Nb_6O_{123})_{\sim 1000}(C_4H_6O_3)_{\sim 5000}$)[57] were prepared in propylene carbonate as reported earlier,[67] with the only modification being that 0.250 g of $[Bu_4N]_5Na_3[(1,5\text{-COD})Ir{\cdot}P_2W_{15}Nb_3O_{62}]$ was used in 3.75 mL of propylene carbonate. After isolation and drying overnight under vacuum, the nanoclusters were stored double-bottled in a N_2-filled drybox until their use.

For each reaction using preformed nanoclusters, the nanoclusters (5.0 mg) were weighed into a predried 2 g glass vial. Then, propylene carbonate (2.5 mL) was added with a 2.5 mL gastight syringe. The solution was agitated with a polyethylene pipet until a homogeneous, light-brown solution characteristic of $Ir(0)_n$ nanoclusters[45] was formed. The solution was then transferred into a new culture tube with a new stir bar, and cyclohexene (0.5 mL) was added with a 1.0 mL gastight syringe. The culture tube was placed in the F-P bottle, which was sealed, brought out of the drybox, and attached to the H_2 line via its Quick-Connects. The nanocluster reaction solution was stirred with the valves to the H_2 line closed (i.e., still under a N_2 atmosphere) while placed in the oil-filled jacketed reaction flask attached to the thermostatted water bath for ≥ 10 min to attain the desired reaction temperature (10–50 °C). To begin each reaction, the F-P bottle was purged 13 times with H_2 (40 ± 1 psig, 15 s/purge). At 5 min after the first purge, the pressure was set at 40 ± 1 psig, $t = 0$ was noted, and pressure versus time data were collected at 2.5 min intervals. The kinetic data were fit with MacKinetics as described in Data Handling.

Attempt To Induce Nanocluster Agglomeration of Isolated $Ir(0)_{\sim 900}$ Nanoclusters Plus Varying Equivalents of $[Bu_4N][BF_4]$. The details of these experiments are described in the Supporting Information.

TEM. TEM analysis was carried out with the expert assistance of Dr. JoAn Hudson at Clemson University. The micrographs were obtained with a Hitachi H7600T microscope operating at 120 keV. Size measurements were obtained from micrographs with 430 000 magnification or higher. Size distributions of nanoclusters were determined by counting >100 nanoclusters. Because propylene carbonate is not a suitable solvent for preparing TEM grids if prepared by placing two drops of the diluted reaction solution onto TEM grids (i.e., a "standard" method[52]), the reaction solutions were sprayed onto TEM grids using an asthmatic's nebulizer (PulmoAide, model 5610D). The nebulizer-prepared TEM grids were prepared in the drybox; specifically, the reaction solution (0.5 mL) was syringed into a new disposable medicine cup, and then 300 mesh silicon monoxide TEM grids (Ted Pella, Inc.) were carefully held with tweezers in front of the nebulizer output for 5 s. The TEM grids were sealed with a PFTE-lined crimp-top cap in a 1.0 mL wide-mouthed GC vial and mailed to Clemson University for analysis.

Data Handling. The MacKinetics freeware used for numerical integration of the agglomeration kinetics was downloaded at http://members.dca.net/leipold/mk/advert.html. The availability and support of MacKinetics has since become problematic, however. Hence, we have listed elsewhere[40] the available numerical integration curve-fitting software that we can locate and are in the midst of collaboration to improve Dynafit,[68] so that it can be used for problems such as the present one.

MacKinetics was used to fit the agglomeration kinetics using isolated and redispersed nanoclusters. Two separate fitting techniques were used to attempt to accurately determine the four rate constants.[39,40] For the first fitting technique, two initial guesses for the rate constants were entered into MacKinetics as fixed values and a full gridsearch was performed to find initial values for the agglomeration rate constants k_3 and k_4 ($B + B \rightarrow C$, rate constant k_3, and $B + C \rightarrow 1.5C$, rate constant k_4,). Then, these two values were used as initial values for the rate constants, and numerical integration was initiated using MacKinetics. Iterations were carried out until the visual fit was good (a qualitative measure, judged by the naked eye) the residual was minimized (≤ 0.01), and the kinetic parameters were self-consistent (i.e., the program returned the final parameters without change from the initially entered parameters). For the second-fitting technique, fitting was carried out using random guesses for the two initial rate constants and no gridsearch was performed. This second technique was employed to avoid local minima, search a maximum amount of parameter space, and estimate the error bars on each parameter. Using the second-fitting technique, each data set was fit ≥ 3 times with three different sets of initial guesses for the parameters. Again, iterations were carried out until the visual fit was good, the residual was minimized, and the kinetic parameters were self-consistent. All $k_{3,obs}$ and $k_{4,obs}$ values were divided by the 1400 stoichiometry factor involved in the pseudo-elementary step to yield the k_3 and k_4 values reported herein (see the Supporting Information for further details).

Acknowledgment. We thank an anonymous referee for very helpful constructive criticism. This work was funded by the Chemical Sciences, Geoscience, and Biosciences Division, Office of Basic Energy Sciences, Office of Science, U.S. Department of Energy Grant DE-FG02-03ER15453.

Supporting Information Available: Table S1, the five criteria for the H_2 reduction of $(Bu_4N)_5Na_3[(1,5\text{-COD})Ir{\cdot}P_2W_{15}Nb_3O_{62}]$ in both acetone and propylene carbonate solvent, showing that there is no change in the mechanism in these two solvents and at least under the stated conditions; details of the pseduo-elementary step method, showing how $-$d[cyclohexene]/dt is connected to the desired measurement of $-$d[B]/dt or $+$d[C]/dt; Figures S1−S5, the raw kinetic data and curve fits for thermal agglomeration and concomitant cyclohexene hydrogenation from 10 to 50 °C; discussion of the deviations from the observed data versus the fits at high conversions/longer times; experimental details and results for nanocluster formation reactions with $(Bu_4N)_5Na_3[(1,5\text{-COD})Ir{\cdot}P_2W_{15}Nb_3O_{62}]$ plus added pyridine and added $[Bu_4N][BF_4]$, for four different anions in acetone and propylene carbonate solvent with added pyridine, and for preformed Ir(0) nanoclusters with added pyridine and added $[Bu_4N][BF_4]$; a section on inducing the four-step mechanism of nucleation, growth, and two types of agglomeration with 44 equiv added pyridine; Figure S6, $P_2W_{15}Nb_3O_{62}^{9-}$-stabilized Ir(0) nanocluster formation reaction in propylene carbonate solvent with 44 equiv pyridine; Table S2, rate constants k_1-k_4 for $P_2W_{15}Nb_3O_{62}^{9-}$-stabilized nanoclusters with added pyridine in propylene carbonate solvent; Table S3, rate constants k_1-k_4 for $P_2W_{15}Nb_3O_{62}^{9-}$-stabilized nanoclusters with 50 equiv added pyridine in propylene carbonate solvent and varying cyclohexene concentrations; Figure S7, cyclohexene hydrogenation by pre-

formed, isolated, and redispersed $P_2W_{15}Nb_3O_{62}^{9-}$-stabilized $Ir(0)_{\sim 900}$ nanoclusters in propylene carbonate in the presence of 0–100 equiv added pyridine; potential problems associated with quantitating the rate constants of the four-step mechanism; discussion regarding the nature of the active catalyst, B versus C. Examination of the apparent activation parameters for Pt(1,5-COD)Cl_2 reduction under H_2. This material is available free of charge via the Internet at http://pubs.acs.org.

CM062001H